JGR Atmospheres

RESEARCH ARTICLE

Key Points:
- The difference between the global downscaled and bottom-up estimates for the whole-city domain exceeds 10% in three of the four cities
- Average grid cell $FFCO_2$ differences at 1-km^2 range from 47% (Salt Lake City) to 84% (LA Basin) with spatial correlations of 0.34 to 0.68
- Average grid cell $FFCO_2$ differences show diminishing agreement improvements when resolution is coarsened beyond 25 km^2

Supporting Information:
- Supporting Information S1

Correspondence to:
K. R. Gurney,
kevin.gurney@nau.edu

Author Contributions:
Conceptualization: Kevin R. Gurney
Formal analysis: Kevin R. Gurney
Funding acquisition: Kevin R. Gurney
Methodology: Kevin R. Gurney
Supervision: Kevin R. Gurney
Writing - original draft: Kevin R. Gurney
Writing – review & editing: Kevin R. Gurney

Comparison of Global Downscaled Versus Bottom-Up Fossil Fuel CO₂ Emissions at the Urban Scale in Four U.S. Urban Areas

Kevin R. Gurney[1,2] (iD), J. Liang[2] (iD), D. O'Keeffe[2], R. Patarasuk[2] (iD), M. Hutchins[2,3], J. Huang[2], P. Rao[4] (iD), and Y. Song[2]

[1]School of Informatics, Computing and Cyber Systems, Northern Arizona University, Flagstaff, Arizona, USA, [2]School of Life Sciences, Arizona State University, Tempe, Arizona, USA, [3]School of Geographical Sciences and Urban Planning, Arizona State University, Tempe, Arizona, USA, [4]School for Environment and Sustainability, University of Michigan, Ann Arbor, Michigan, USA

Abstract Spatiotemporally resolved urban fossil fuel CO_2 ($FFCO_2$) emissions are critical to urban carbon cycle research and urban climate policy. Two general scientific approaches have been taken to estimate spatiotemporally explicit urban $FFCO_2$ fluxes, referred to here as "downscaling" and "bottom-up." Bottom-up approaches can specifically characterize the CO_2-emitting infrastructure in cities but are labor-intensive to build and currently available in few U.S. cities. Downscaling approaches, often available globally, require proxy information to allocate or distribute emissions resulting in additional uncertainty. We present a comparison of a downscaled $FFCO_2$ emission data product (Open-source Data Inventory for Anthropogenic CO_2 (ODIAC)) to a bottom-up estimate (Hestia) in four U.S. urban areas in an effort to better isolate and understand differences between the approaches. We find whole-city differences ranging from −1.5% (Los Angeles Basin) to +20.8% (Salt Lake City). At the 1 km × 1 km spatial scale, comparisons reveal a low-emission limit in ODIAC driven by saturation of the nighttime light spatial proxy. At this resolution, the median difference between the two approaches ranged from 47 to 84% depending upon city with correlations ranging from 0.34 to 0.68. The largest discrepancies were found for large point sources and the on-road sector, suggesting that downscaled $FFCO_2$ data products could be improved by incorporating independent large point-source estimates and estimating on-road sources with a relevant spatial surrogate. Progressively coarsening the spatial resolution improves agreement but greater than approximately 25 km^2, there were diminishing returns to agreement suggesting a practical resolution when using downscaled approaches.

Plain Language Summary Comparison of greenhouse gas emission approaches using globally available data in specific cities shows large differences when compared to greenhouse gas emission approaches constructed from local data sources. Differences are largest at the smaller scales compared to the whole city. This suggests a limit on the use of global greenhouse gas inventories when applied to urban areas.

1. Introduction

Fossil fuel carbon dioxide ($FFCO_2$) emissions, the dominant anthropogenic greenhouse gas, are not only the largest annual net flux of CO_2 to the atmosphere but have been steadily increasing since the Industrial Revolution (Hartmann, 1998; Le Quéré et al., 2013). A complete understanding of the key components of the global carbon budget and their interactions cannot be achieved without accurate estimation of $FFCO_2$ emissions. Traditionally, quantification of $FFCO_2$ emissions was accomplished at national spatial scales and annual temporal scales using statistics on energy consumption and trade (Andres et al., 1999; Boden et al., 1995; Macknick, 2011; Marland et al., 1985). However, as CO_2 measurement and modeling systems increased in complexity and interest moved from global to national and regional understanding, there has been an increasing need for $FFCO_2$ emission data products at higher spatiotemporal resolution and in regularized or gridded formats (Andres et al., 1996; Asefi-Najafabady et al., 2014; Doll et al., 2000; Erickson et al., 2008; Gately & Hutyra, 2017; Ghosh et al., 2010; Gregg et al., 2009; Gregg & Andres, 2008; Gurney et al., 2009; Nassar et al., 2013; Oda & Maksyutov, 2011; Olivier et al., 1999; Ou et al., 2015; Rayner et al., 2010; Wang et al., 2013). For example, spatiotemporally resolved $FFCO_2$ emissions are a necessary additional constraint to atmospheric CO_2 inversions/data assimilation systems which infer surface fluxes by integrating atmospheric CO_2 measurements, atmospheric transport simulations, and a

priori flux estimates (e.g., Gurney et al., 2002, 2005; Enting, 2002; Liu et al., 2017; Schuh et al., 2010). Furthermore, the emergence of subnational policy actors has also placed additional emphasis on quantifying $FFCO_2$ emissions at finer space and time scales than traditional national/annual inventories (Bulkeley, 2010; Gurney et al., 2015; Hsu et al., 2017; Hutyra et al., 2014). Examples of these global spatiotemporally resolved $FFCO_2$ emission data products include the Carbon Dioxide Information and Analysis Center (CDIAC) data product (Boden et al., 2017), the Emission Database for Global Atmospheric Research (EDGAR) data product (Janssens-Maenhout et al., 2012), and the Open-source Data Inventory for Anthropogenic CO_2 (ODIAC) data product (Oda & Maksyutov, 2011; Oda et al., 2018). Some of the estimation systems rely on optimization routines that solve a model of $FFCO_2$ emissions subject to remote-sensing constraints, such as the Fossil Fuel Data Assimilation System (Asefi-Najafabady et al., 2014; Rayner et al., 2010). These efforts are typically resolved at spatial scales from $1 \times 1°$ down to $0.01 \times 0.01°$ and resolve time at annual to hourly time scales.

In the last decade, the trend toward increased resolution has continued with research advancing $FFCO_2$ emission estimation able to resolve subcity emissions and activity (Gurney, 2014; Hutyra et al., 2014). This owes in large part to the fact that about 70% of global CO_2 emissions are produced in urban areas which occupy less than 1% of the Earth's land area (Seto et al., 2015). Motivated by these numerical realities and the recognition that low-emission development is consistent with a variety of other co-benefits (e.g., air quality improvement), cities are taking steps to mitigate their CO_2 emissions (Hsu et al., 2015; Rosenzweig et al., 2010; Watts, 2017). For example, 9,120 cities representing over 770 million people (10.5% of global population) have committed to the Global Covenant of Mayors to promote and support action to combat climate change (Global Covenant of Mayors (GCoM), 2018).

Spatiotemporally resolved $FFCO_2$ estimation systems have similarly transitioned to the urban scale to support the increased need of cities and to better understand aspects of the urban carbon cycle and urban science (Brioude et al., 2013; Duren & Miller, 2012; Feng et al., 2016; Lauvaux et al., 2016; McKain et al., 2012; Mitchell et al., 2018; Turnbull et al., 2015; Wu et al., 2016). For example, urban estimation systems that combine atmospheric monitoring, transport models, and bottom-up emission constraints require information in a spatially explicit format. Because atmospheric monitoring in cities is a direct reflection of specific upwind sources modified by spatially dependent atmospheric transport, the constraint provided by bottom-up estimation must also be spatially explicit and at scales of 1 km^2 or finer to resolve in situ urban atmospheric CO_2 observations.

Equally important, as urban greenhouse gas emission mitigation policy migrates from long-term pledges to concrete action, policy effectiveness will mandate prioritizing emitting targets by magnitude and or reduction potential per unit effort expended (Gurney et al., 2015). This will require spatial and functional specificity. For example, knowing that a small portion of road surface accounts for a large share of total on-road $FFCO_2$ emissions (a typical reflection of the distribution of emissions in cities) will be critical knowledge to guide reduction efforts to those places and conditions where reductions can be achieved first with the least amount of cost or effort (Patarasuk et al., 2016).

It is worth noting that there is a long history of whole-city carbon footprint estimation using a number of different methodological approaches and accounting frameworks (e.g., Kennedy et al., 2009; Ramaswami et al., 2008; Zhao et al., 2011). In addition to the work described in the scientific literature, there are many estimates in the gray literature performed by city staff or nongovernmental organizations (e.g., Goodfriend et al., 2017). While these efforts remain important for policy application, the focus in this study is on subcity spatially resolved efforts from the peer-reviewed literature. This is driven, in part, by the need to focus on estimation approaches, such as the science-driven, spatiotemporal explicit $FFCO_2$ emission data products discussed in this study that can be linked to atmospheric observing systems.

Spatiotemporally resolved $FFCO_2$ emission data products from the global to the urban are developed using two general approaches which we refer to here as "bottom-up" and "downscaling." Bottom-up approaches use direct flux monitoring and sectoral activity data gathered from various socioeconomic sources to develop spatiotemporally explicit, mechanistic $FFCO_2$ emissions (Brondfield et al., 2012; Gately et al., 2013; Gately & Hutyra, 2017; Gurney et al., 2009; Jones & Kammen, 2014; Parshall et al., 2010; Patarasuk et al., 2016; Pincetl et al., 2014; Porse et al., 2016; Shu & Lam, 2011; VandeWeghe & Kennedy, 2007; Zhou & Gurney, 2010). At

the urban scale, this approach has been pioneered by the Hestia Project which estimates $FFCO_2$ emissions for urban landscapes at the building/street spatial scale and hourly temporal scale with sectoral, fuel, and functional details (Gurney et al., 2012).

Downscaling approaches, by contrast, use spatial surrogates such as population data and commercial business hours to distribute global or national total emissions over a defined space and time domain (Andres et al., 2012). For example, the CDIAC $1 \times 1°$ inventory used population density to distribute national $FFCO_2$ emissions to a gridded form (Andres et al., 1996). Some emission data products can be considered hybrids of these two approaches reflecting mixtures of bottom-up and downscaling elements. For example, Fossil Fuel Data Assimilation System uses a database of powerplant $FFCO_2$ emissions in combination with optimization procedures to downscale remaining emitting sectors using population and nighttime lights (Asefi-Najafabady et al., 2014).

In comparison to downscaling approaches, bottom-up approaches usually have higher spatial resolution and explicit sectoral representation. Nevertheless, constructing a bottom-up data product requires lengthy development times, and thus are available only in a few U.S. cities. This means, outside of a few U.S. urban areas, downscaling-derived $FFCO_2$ emission data products are the only option available to urban carbon scientists and policy researchers.

The uncertainty associated with spatiotemporally resolved $FFCO_2$ emission data products is critical to both scientific and policy application. For example, when these uncertainties are included as part of the prior emission constraint in atmospheric CO_2 inversions, the uncertainties will propagate and contribute to the posterior flux errors. Traditionally, prior $FFCO_2$ emissions have been incorporated into inversions with no prior uncertainty, risking the aliasing of error (including biases) into posterior estimates of other components of the carbon cycle (Engelen et al., 2002; Gurney et al., 2005; Shiga et al., 2014; Zhang et al., 2015).

Attempts have been made to quantify the uncertainty of global downscaled $FFCO_2$ estimation approaches. The uncertainty is often divided into two distinct components: (1) magnitude uncertainty associated with the predownscaled emissions, such as provided by national fuel consumption accounts (Macknick, 2011), and (2) disaggregation uncertainty such as that associated with the downscaling process in its reliance on imperfect or unrepresentative spatial proxies (e.g., Hogue et al., 2016). Uncertainty is estimated directly from elements or techniques used to generate the data product (Andres et al., 2016) and via intercomparison among different data products as a guide to estimation uncertainty (Hutchins et al., 2016). For example, Andres et al. (2016) estimated uncertainty associated with the CDIAC $1° \times 1°$ $FFCO_2$ emission data product by examining multiple contributions (e.g., use of proxy spatialization, magnitude) to error finding an average grid cell uncertainty of $\pm120\%$ (2σ). In a similar study using a slight modification to the CDIAC $1° \times 1°$ data product, Hogue et al. (2016) estimated a larger uncertainty in the United States of $\pm120\%$ (1σ) at the scale of an individual grid cell. Asefi-Najafabady et al. (2014) generated a formal Bayesian posterior uncertainty estimate associated with the $0.1° \times 0.1°$ resolution Fossil Fuel Data Assimilation System $FFCO_2$ emission data product, reporting an average grid cell-scale uncertainty of 30% (1σ). Gately and Hutyra (2017) compared a number of global gridded $FFCO_2$ emission data products to each other and a regional bottom-up $FFCO_2$ emission data product (ACES) finding differences exceeding 100% for half of the grid cells in the northeastern U.S. domain. These uncertainty estimates are difficult to compare in that they use different approaches, include different components of uncertainty, and most importantly are reporting from uncertainty distributions that are not normally distributed making the estimation of an average an imprecise metric.

With these efforts as context, this paper takes another step toward uncertainty characterization through a comparison at the urban scale between a bottom-up $FFCO_2$ emission data product, represented by the Hestia Project, and a downscaled data product, ODIAC2013a. Both approaches used here do not include biosphere fluxes (also important to quantify in cities) and hence, focus on the fossil fuel combustion only. ODIAC is of particular interest among the available global data products because it is produced at high resolution and has been used in numerous urban emission studies (Brioude et al., 2013; Lauvaux et al., 2016; Oda et al., 2017). Specifically, this paper asks three research questions: (1) What is a "proxy" (derived as a difference to the bottom-up emissions) uncertainty estimate of the downscaled $FFCO_2$ emissions at the urban scale; both for whole-city and at the 1 km^2 spatial scale? (2) At what spatial resolution do the bottom-up and downscaled $FFCO_2$ emissions best agree; (3) What can be done to further improve global downscaled $FFCO_2$ emission data products within the urban carbon cycle context?

2. Data and Methods

Multiple statistical metrics and graphical representations were employed to characterize the differences between the bottom-up and downscaled urban $FFCO_2$ emission estimation approaches. We start with an overview of the two data products with respect to their development methods and specifications, and then present the rationale for the choice of comparison metrics.

2.1. Downscaled $FFCO_2$ Emissions

The downscaled $FFCO_2$ emission data product used in this study, ODIAC2013a, is a 1 km × 1 km global fossil fuel CO_2 emission data product developed by assembling preexisting data sets including a national total emission database, a powerplant database, and the Defense Meteorological Satellite Program/Operational Linescane System nightlight imagery (Oda & Maksyutov, 2011). The ODIAC2013a methodology uses annual total emissions by country from the Carbon Dioxide Information Analysis Center (Boden et al., 2013) extended beyond the year 2009 using additional data from British Petroleum. The Carbon Monitoring for Action (CARMA) power plants database, providing information about the carbon dioxide emissions and location of more than 60,000 power plants in over 200 countries, a portion of which was used in ODIAC to characterize the emissions associated with large electricity producers (Ummel, 2012). To obtain national emissions for the sources other than electricity production, the powerplant emissions were subtracted from the national totals and the resulting emissions spatially distributed from country to grid cells in proportion to their nightlight radiance value. Hence, for the land-based U.S. case we are considering in this study, the nightlight downscaling accounts for the majority (nationally, roughly 56%) of 2011 U.S. $FFCO_2$ emissions (USEPA, 2017). This is a minimum percentage as urban areas do not typically contain electricity production facilities within the urban boundary. For example, in the city of Indianapolis, the percentage that would rely on downscaling rises to 70% of the 2002 total (Gurney et al., 2012). The ODIAC 2013a data product did not provide uncertainty estimates with the emissions. However, more recent releases of the data product include national-scale uncertainty, but were not available at the time analysis was completed (November 2015) in the current study.

2.2. Bottom-Up $FFCO_2$ Emissions

The bottom-up $FFCO_2$ emission data product used here, Hestia, quantifies urban $FFCO_2$ emissions to the individual building/street segment spatial scales and hourly temporal scales (Gurney et al., 2012; Zhou & Gurney, 2010). Begun in the mid-2000s, the Hestia Project has now made high-resolution $FFCO_2$ estimates for the Los Angeles Basin (Newman et al., 2016), Indianapolis (Gurney et al., 2012, 2017), Salt Lake City (Patarasuk et al., 2016), and Baltimore (Gurney et al., 2012; see supporting information). These four urban areas are used for comparison with the ODIAC2013a $FFCO_2$ emission data product.

Hestia uses a large collection of data and modeling techniques to determine $FFCO_2$ fluxes including regulated air pollution flux reporting, socioeconomic data, CO_2 flux monitoring, building energy simulation, and traffic monitoring. Hestia quantifies emissions at the spatial scale of individual emission stacks, buildings, land parcels, and roadways. Hence, it represents these emitting entities as points, polylines, and polygons. The Hestia $FFCO_2$ emissions are also categorized by economic sector (e.g., residential, commercial, onroad) and the spatial representation and sector are coupled. For example, the on-road $FFCO_2$ emissions are represented on polyline segments while the commercial, residential, and industrial sector emissions are represented as polygon-shaped sources (indicative of parcels of land or individual buildings). Hestia emissions can be gridded to various grid resolutions from 200 to 1,000 m to serve different applications.

The Hestia methodology is provided in Gurney et al. (2012). Uncertainty estimation for the Hestia results are challenging owing to the fact that many of the data sets used to construct the flux results are not accompanied by uncertainty or traceable to transparent sources or methods. Hence, for the purposes here we use a combination of expert judgment and analysis from one of the four urban areas considered in this study. The only existing approach to analytical objective evaluation is in comparison to atmospheric CO_2 inversion studies. Though not immune to biases itself (e.g., transport errors, misspecification of prior biosphere fluxes), atmospheric CO_2 inversion research has been accomplished in the city of Indianapolis and the results show agreement with the Hestia $FFCO_2$ emissions within 3.3% (CI −4.6 to +10.7%; Gurney et al., 2017). This suggests both potential bias (3.3%) and an estimation uncertainty (~7.5%).

Further uncertainty considerations at the scale of an individual grid cell are based on a combination of existing analysis of subcomponents of the $FFCO_2$ emission estimation and expert judgment. Gurney et al. (2016) compared two powerplant emission estimation data sets, finding that one fifth of the facilities had monthly $FFCO_2$ emission differences exceeding −6.4/+6.8% for the year 2009 (the closest analyzed year to the 2011 analysis examined here). Other component fluxes in the Hestia estimation procedure are strongly driven by the CO and CO_2 emission factors specific to fuel and sector. Examination of the range of emission factors conservatively places the uncertainty at 20% based on our expert judgment (see supporting information).

Hence, we combine these uncertainty values and estimate a 95% confidence interval at the whole-city scale of 11% and an individual grid cell uncertainty of 25%. These would be equivalent to standard errors of 5.5 and 10% at the whole city and grid cell-scale, respectively. Work is underway that includes a complete input parameter range for the Hestia emission data results to more formally assign uncertainty at multiple scales and for each urban domain individually.

2.3. Methods

For each of the four urban areas, the Hestia total emissions including all sectors were gridded at $1 \text{ km} \times 1 \text{ km}$ spatial resolution ($0.0083° \times 0.0083°$) in conformance with the ODIAC spatial grid (Figure 1).

Six comparison metrics were used to quantify differences between the two data products (Table 1). These measures of difference include whole-city and grid cell-scale metrics in addition to differences in spatial distribution. The whole-city total relative difference, *TRD*, is calculated as (ODIAC − Hestia)/Hestia × 100%. The summed absolute difference, *SAD*, is the sum of the grid cell-scale absolute differences integrated over the entire city. This is also normalized to the whole-city emissions to achieve the SAD as a fraction of total emissions, *SADFD*, using the Hestia total in the denominator. We include the spatial correlation, *SC*, a metric independent of magnitude (Rayner et al., 2010). This is calculated as the Pearson's *R* across all paired grid cells in the two data products. As spatial correlations are sensitive to extreme values, the two data products were subjected to an extreme value removal process in which values greater than the sum of the mean and 3 standard deviations were excluded prior to spatial correlation estimation. In order to maintain alignment between the two data products, if a value in either was removed, its counterpart was also removed resulting in the removal of 79 matching grid cells (across the four urban domains).

Similar to the whole-city total relative difference, we define the grid cell-scale relative difference (*GRD*). The grid cell absolute median percent difference, *GAMRD*, is the median of a set of individual paired grid cell relative differences, where the differences are represented in absolute units (i.e., so all GRD values are positive). This metric, in particular, will be used to generate a "proxy" uncertainty measure for the ODIAC data product.

3. Results

The whole-city relative emission difference (TRD) between the ODIAC and Hestia $FFCO_2$ emission estimates across the four urban areas range from −1.52% (Los Angeles Basin) to +20.82% (Salt Lake City; Table 2). In all but the Los Angeles Basin, the difference is positive, indicating that the ODIAC result is larger than the Hestia whole-city estimate. Furthermore, other than for the Los Angeles Basin, the difference between the two approaches exceeds the 95% confidence internal assigned to the Hestia whole-city estimates implying that these whole-city differences are statistically significant at two standard errors.

In addition to differences at the whole-city scale, there are differences in spatial distribution. The spatial correlation (SC) value for Salt Lake City is the largest among the four urban areas suggesting the greatest agreement in spatial distribution. However, it also has the largest TD value combined with a relatively moderate SADFD value, suggesting that there is a whole-city offset between the two data products though the spatial distribution is similar. Baltimore, by contrast, exhibits a low SC value but a relatively large SADFD, suggesting poor spatial correspondence overall. The Los Angeles Basin shows the largest SADFD value with a relatively large SC value among the four cities. This suggests reasonable spatial agreement but likely a small number of grid cells with large differences. Given the agreement in TRD, this suggests that these grid cell differences are of both positive and negative magnitude, canceling in the estimation of the total (but not in the SADFD).
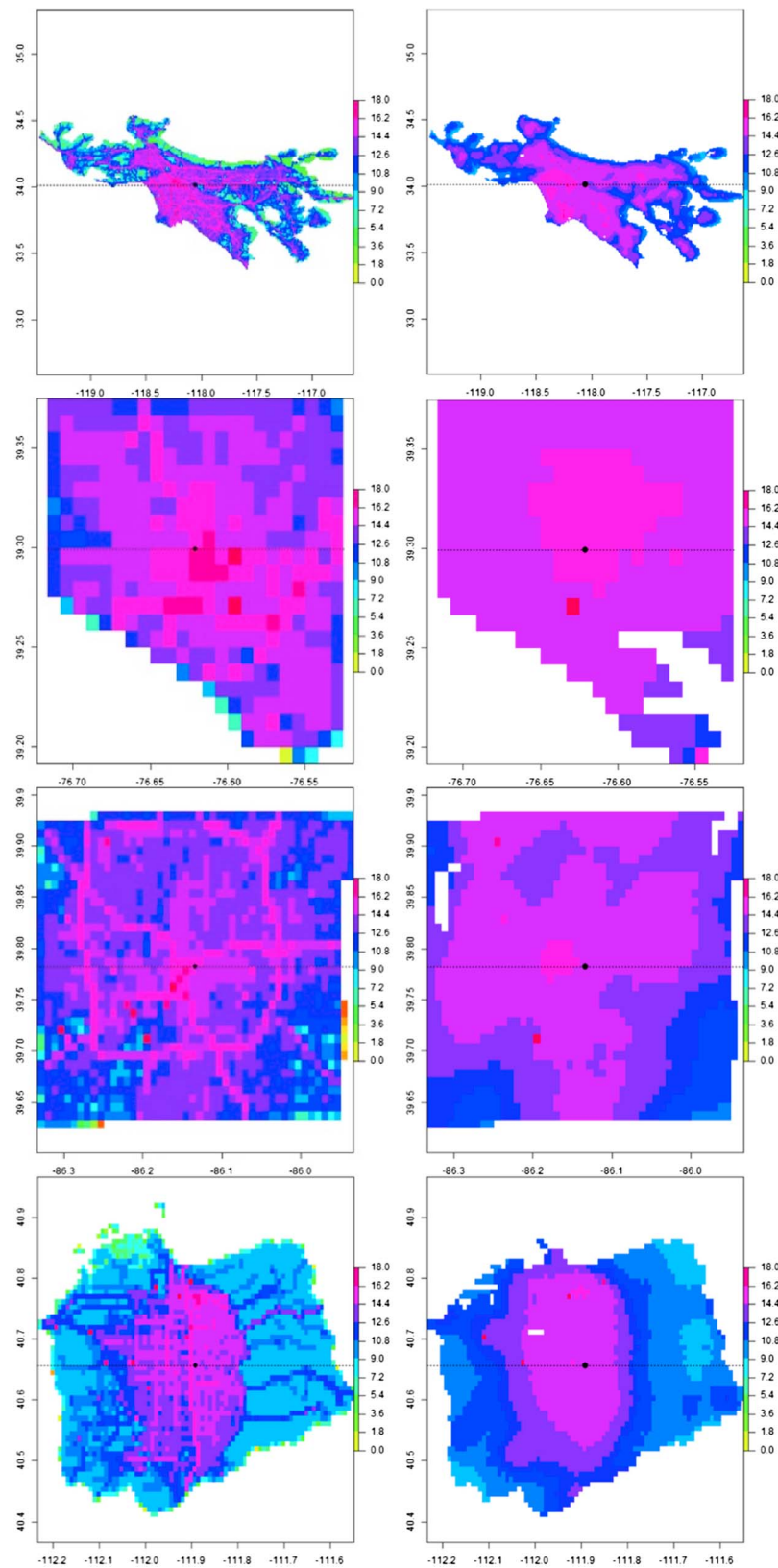
Figure 1. Spatial distribution of 1 km × 1 km annual $FFCO_2$ emissions in the four U.S. cities included in this study. The rows list the cities as Los Angeles Basin, Baltimore, Indianapolis, and Salt Lake City. The columns represent (left) Hestia $FFCO_2$ emissions and (right) ODIAC2013a $FFCO_2$ emissions. Units: natural logarithm kg C/grid cell.

Table 1
List of Statistical Metrics Used to Compare a Downscaled to Bottom-Up FFCO$_2$ Emission Data Product in the Four Urban Areas

No.	Metric
1	Whole-city relative difference (TRD) in percent (Table 2)
2	Summed absolute difference (SAD; Table 2)
3	SAD as fraction of total emissions (SADFD) in percent (Table 2)
4	Spatial correlation coefficient (SC; Table 2)
5	Grid cell relative difference (GRD) in percent (Figure 3)
6	Grid cell absolute median percent difference (GAMRD; Figure 3)

Note. Table/figure where results can be found are included.

At the individual grid cell spatial scale, Hestia exhibits a larger range of values across all urban areas (Figure 2). Regressing the two grid cell-scale data sets results in positive slope values ranging from a minimum of 0.15 (Baltimore) to a maximum of 0.61 (Salt Lake City) with coefficients of determination (R) values ranging from 0.41 (CI 0.306, 0.512; Baltimore) to 0.78 (CI 0.764, 0.799; Salt Lake City). This suggests broad agreement in the directionality of small to large emitting grid cells but a difference in emission range.

The Los Angeles Basin comparison shows a somewhat nonlinear relationship or two different correlated relationships at the larger and smaller end of the emission distribution in a fashion similar to the comparison in Salt Lake City. A large number of emitting grid cells at the upper and lower extremes of the range of values deviate from the general agreement between the two emission data products. These instances are particularly evident in the Los Angeles Basin and Salt Lake City and to a lesser degree in Indianapolis. There appears to be better agreement for the larger values across all the urban areas with greater disagreement for the smaller emitting grid cells. It is worth noting that Figure 2 reveals a conspicuous lower threshold value in the ODIAC data product, possibly related to the nightlight saturation effect (Levin & Duke, 2012) which suppresses the range of values. This is particularly notable in the Los Angeles Basin and Salt Lake City where the lower values are cut off at approximately 22,000 kg C/grid cell/year (the natural logarithm of 22,000 = 10). In Baltimore, the ODIAC data product shows few emission values toward the low end of the numerical distribution, which could be partially responsible for the shallow regression slope. The ODIAC FFCO$_2$ emissions in the other three urban areas, by contrast, tend to have a wider range of values from 10 to 20 Tg C/grid cell/year, which could have led to the steeper slopes.

To highlight the spatial differences, Figure 3 shows the relative difference calculated at the scale of individual 1 km × 1 km grid cells (GRD: ($ODIAC_i − Hestia_i$)/$Hestia_i$ × 100%). Large positive and negative values occupy a significant proportion of the space in each of the urban area difference maps. In Indianapolis, the Los Angeles Basin, and Salt Lake City, large negative GRD values are coincident with the road network. These large negative GRD values suggest higher emission intensities along roads in the Hestia versus ODIAC emissions. In Salt Lake City, there is a cluster of large negative GRD values in the northwestern corner bordering the Great Salt Lake. This is likely due to the Hestia distribution of nonroad FFCO$_2$ emissions which, in the Salt Lake City case, are evenly distributed within a census block group versus ODIAC's use of nighttime lights for all emissions other than power plants. Nevertheless, it should be noted that the FFCO$_2$ emissions in this area of SLC are small in magnitude, as seen in Figure 1. The southeastern portion of Baltimore also exhibits a cluster of large negative GRD values. This is coincident with commercial marine vessel activity in the Hestia results. Large positive GRD values appear clustered in the lower density or suburban regions across all four urban areas. As ODIAC emissions are allocated to artificial light intensity during nighttime hours when building fuel combustion (i.e., for heating) is at a minimum but lighting at a maximum (for which Hestia emissions are located at electricity production facilities), ODIAC overestimation may be occurring. The 79 extreme difference values removed prior to the Pearson R correlation calculation individually noted in Figure 3.

Table 2
Total 2011 Urban Emissions, Whole-City Relative Difference (TRD), Summed Absolute Difference (SAD), SAD as Fraction of Whole-City Hestia Emissions (SADFD), and Spatial Correlation (SC) Across Four Urban Areas When Comparing a Global Downscaled (ODIAC2013a) Data Product to a Bottom-Up (Hestia) Data Product

Urban Area	Area (km^2)	ODIAC Total (Tg C/year)	Hestia Total (Tg C/year)	TRD (%)	SAD (Tg C/year)	SADFD	SC
Los Angeles Basin	17,795	32.89	33.39 (29.8, 37.0)	−1.52%	21.3 (19.0, 23.6)	0.63	0.51 (0.48, 0.54)
Salt Lake City	3,190	3.83	3.17 (2.83, 3.51)	20.8%	1.54 (1.37, 1.71)	0.49	0.68 (0.62, 0.72)
Indianapolis	1,681	3.53	4.03 (3.60, 4.46)	12.5%	1.85 (1.65, 2.05)	0.46	0.34 (0.19, 0.46)
Baltimore	404	1.43	1.29 (1.15, 1.43)	10.7%	0.70 (0.62, 0.78)	0.54	0.34 (0.23, 0.45)

Note. Values in parentheses represent the 95% confidence interval from the bottom-up (Hestia) results.
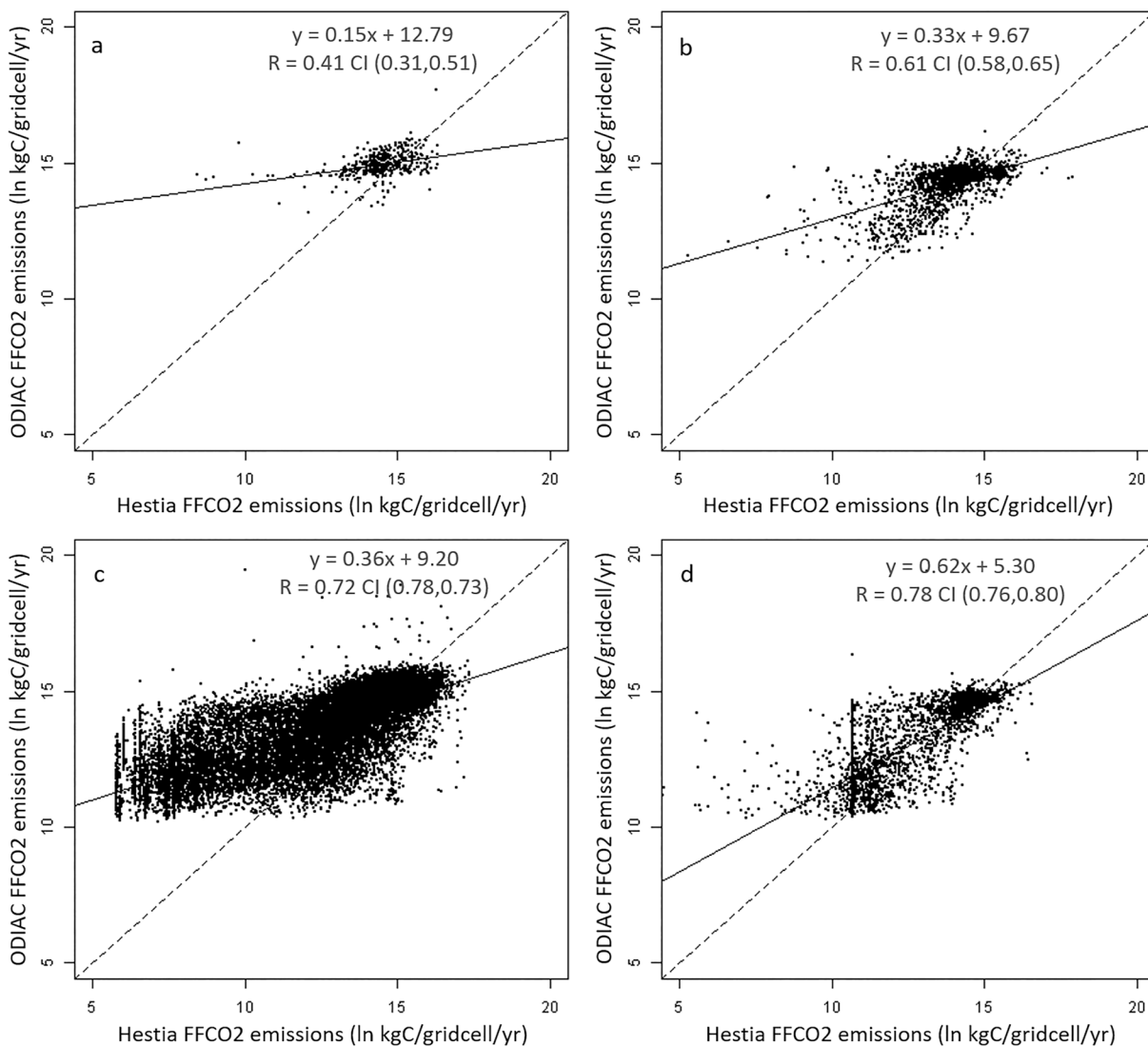
Figure 2. Comparison of annual ODIAC and Hestia $FFCO_2$ emissions at 1 km × 1 km spatial resolution in the four U.S. urban areas: (a) Baltimore, (b) Indianapolis, (c) the Los Angeles Basin, and (d) Salt Lake City. Units: natural logarithm kg C/grid cell/year.

Figure 4 shows the frequency distribution of the gridded 1 km × 1 km $FFCO_2$ emissions for the two emission data products across the four urban areas. The ODIAC $FFCO_2$ emission values have a narrower range than the Hestia results, largely limited to 2.2×10^4 to 8.8×10^6 kg C/grid cell/year, consistent with Figure 2. The peak values across the four urban areas in the Hestia emissions are generally associated with smaller emission magnitudes. In Baltimore, Indianapolis, and the Los Angeles Basin, the ODIAC results show roughly twice the occurrence of the maximum emission values. In Salt Lake City, by contrast, both emission data products show a bimodal distribution in which Hestia shows a greater frequency of the small maxima while ODIAC shows a greater frequency of the large maxima. This is consistent with the bimodal distribution noted in Figure 2 for Salt Lake City. The distribution for Los Angeles Basin also shows a bimodal distribution in both data products, although the magnitude of the secondary maxima is less prominent and the two centers of agreement less distinct.

Because mean values of the grid cell-scale comparison (i.e., the GRD values) are sensitive to large percent differences composed of small absolute grid cell emissions (and vice versa) and sign cancelation of those same GRD values, the grid cell absolute median relative difference (GAMRD) statistic attempts to isolate a single metric of the grid cell ensemble differences. We examined the GAMRD as a function of the Hestia $FFCO_2$ cumulative distribution function using a descending rank order of emitting grid cells
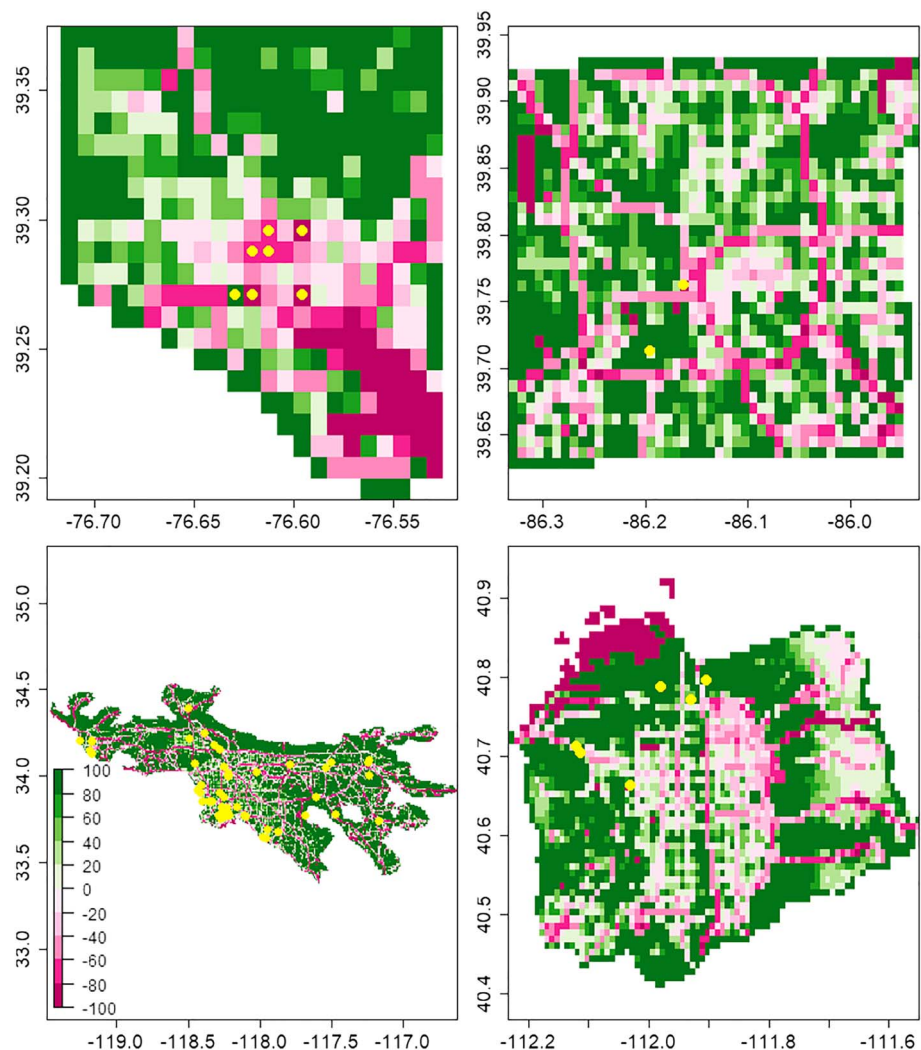
Figure 3. Annual grid cell FFCO$_2$ emission relative difference (GRD) between the Hestia and ODIAC emissions at 1 km × 1 km spatial resolution (GRD: ODIAC$_i$ − Hestia$_i$)/Hestia$_i$ × 100%) in four U.S. urban areas: (a) Baltimore, (b) Indianapolis, (c) the Los Angeles Basin, and (d) Salt Lake City. Yellow circles denote 79 large individual difference values.

(Figure 5) exploring whether or not the GAMRD shows sensitivity to the extreme ends of the magnitude distribution. Between 10 and 90% of the accumulated FFCO$_2$ emissions, the GAMRD values, across all four urban areas, have lesser variance. In all but Salt Lake City, the GAMRD value is between 40 and 75% with Salt Lake City varying between 30 and 60%. The grid cells in the last 10% of the accumulation (large percent difference but small magnitude emissions) show unstable GAMRD values, especially in Salt Lake City and the Los Angeles Basin, due to a large number of small-emitting grid cells with GAMRD values exceeding 100%. These are not representative of the general grid cell-scale differences between the two data products but reflect the influence of the tails of the distribution of percent differences between the two approaches. This suggests that at accumulations at or below 90%, the general mean differences can be encapsulated in a somewhat consistent GAMRD value. In the four cities examined here, the GAMRD ranges from 45% (Salt Lake City) to 67% (Los Angeles Basin) at the 90% threshold value.

The precision of gridded FFCO$_2$ emissions can be systematically related to the spatial resolution (Liang et al., 2017). Given the heterogeneity of the urban emission landscape, aggregating from fine to coarse resolution may smooth or average over the spatial variation potentially leading to fewer differences between the bottom-up and downscaled emission approaches. We examine the three spatial metrics (SC, SAD, GAMRD) across a gradient of spatial resolution considering only those grid cells below the 90% cumulative distribution threshold described in Figure 5. Of the four urban domains, only the Los Angeles Basin is of
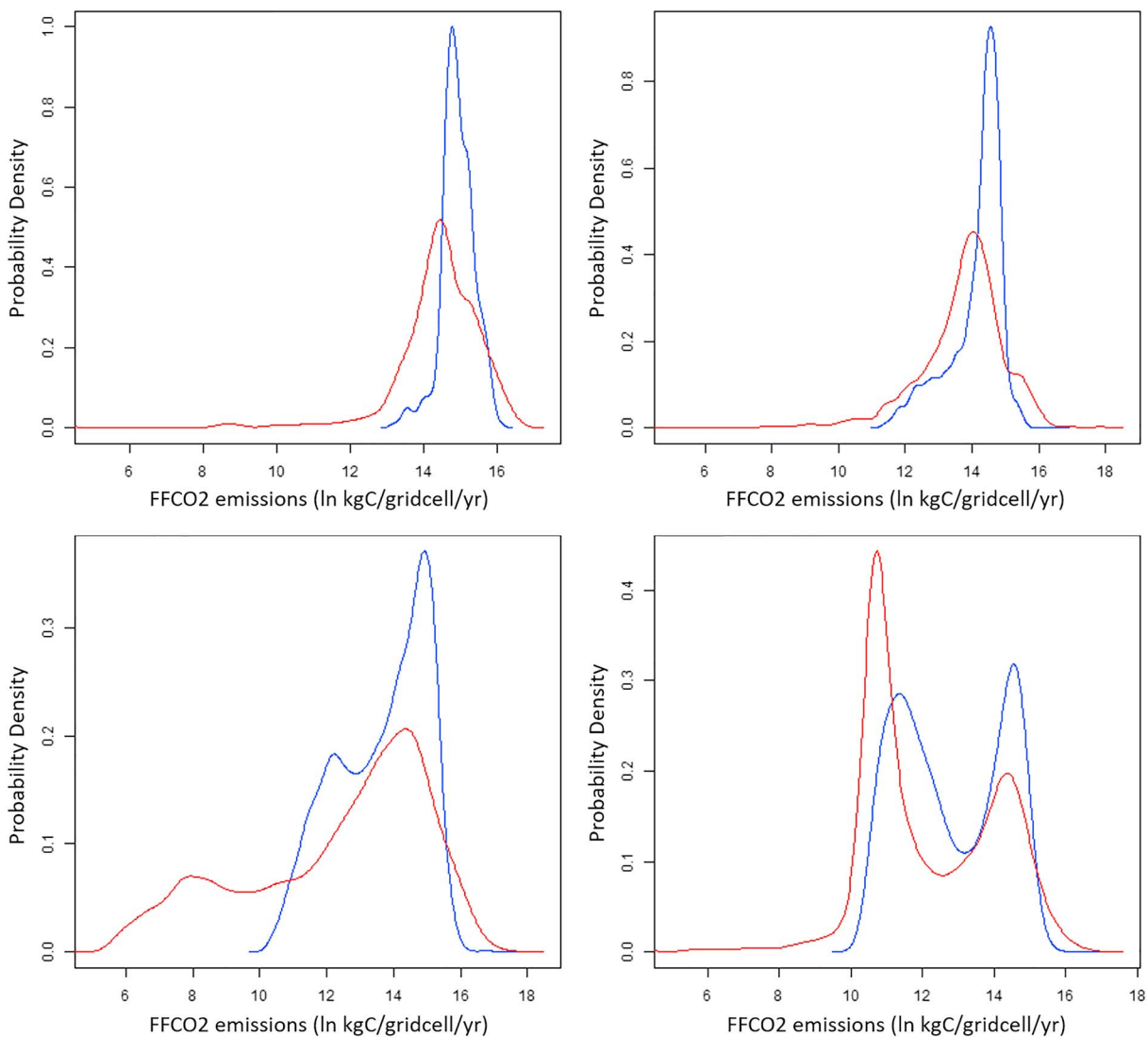
Figure 4. Probability density function of annual 1 km × 1 km FFCO$_2$ emissions for the ODIAC (blue line) and Hestia (red line) approaches in four U.S. urban areas: (a) Baltimore, (b) Indianapolis, (c) the Los Angeles Basin, and (d) Salt Lake City. Units: natural logarithm kg C/grid cell/year.

sufficient size to offer an adequate range to highlight the changes in spatial difference as the spatial resolution of ODIAC is coarsened (Figure 6). As the spatial resolution is coarsened from 1 km × 1 km to 13 km × 13 km (169 km^2), the SAD and GAMRD metrics decline and the SC value increases in a near-inverse manner. For example, the SC increases from 0.61- at the 1-km^2 spatial resolution to 0.93 at a spatial resolution of 13 km × 13 km, whereas the SAD decreases from 16.7 to 6.1, respectively (Figure 6b). The GAMRD value declines from 55% at 1 km^2 to roughly 20% at 13 km × 13 km. There is asymptotic behavior in all three metrics as the spatial resolution is coarsened and a calculation of the first derivative ($|dy/dx|$) of each metric suggests diminishing returns to agreement when coarsening the resolution. The initial turnover point (minimum first derivative) is at 5 km × 5 km (25 km^2) in all three metrics. Although there is continued improvement in agreement, further improvements proportionately decline at coarser resolutions.

Correlation between the ODIAC and Hestia FFCO$_2$ emission data products is sensitive to a small set of extreme difference values. We paired the extreme values (greater than 3 standard deviations from the mean), in each of the four urban areas by visually inspecting these extreme values against street maps and high-
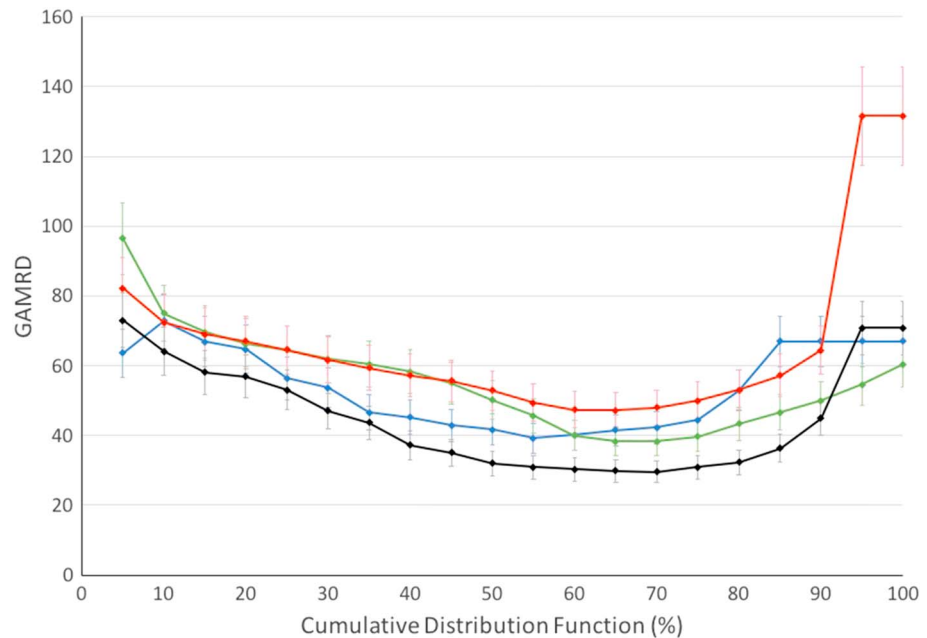
Figure 5. The grid cell median absolute percentage difference (GAMRD) versus the Hestia annual FFCO$_2$ emission cumulative distribution function across the four urban areas at a resolution of 1 km × 1 km. Baltimore (blue), Indianapolis (green), Los Angeles (red), and Salt Lake City (black). The x axis bins represent sampling the results in 5% increments.

resolution satellite imagery. We linked each ODIAC grid cell with a Hestia grid cell counterpart (when not obviously coincident) in an attempt to isolate the potential source of difference. Point sources in the Hestia estimate were geocoded via self-reported air quality reporting and further inspected and corrected with manual inspection. These locations, therefore, can serve as ground-truth positions. These 79 pairs of extreme values were placed into one of four categories: (1) the values in the two data products share the same grid cell, (2) the values are within three grid cells of each other, (3) the value in the Hestia data product has no nearby partner in the ODIAC data product, and (4) vice versa.

Of all the extreme difference values identified, 35.4% were associated with category (1) and had mean GRD values as high as 87%. For the grid cells associated with category (2), electricity production was the predominant emitting sector. This suggests that there may be issues of data quality related to the global power plant database used by ODIAC2013a which are mostly magnitude related but also related to incorrect geolocation in a few cases. For the category (3) and (4) cases, which, respectively, account for 50.6 and 8.9% outliers, the dominant emitters consist of a mixture of industrial facilities, airports, and power plants.

There are a number of cases in which large GRD values are associated with large FFCO$_2$ emissions in both approaches. For example, the grid cell associated with the West Valley Generation Project Powerplant (40.66, −112.03) in Salt Lake City shows emissions of 9.73×10^7 kg C/year in the ODIAC results (which relied upon the CARMA database), more than 3 times larger than the Hestia emissions of 2.96×10^7 kg C/year (retrieved from the United States Environmental Protection Agency continuous emission monitoring records). Similar inconsistencies appear to be present in grid cells dominated by airport emissions. For example, the grid cell that contains the Los Angeles International Airport (LA Basin 33.94, −118.41) emits 3.37×10^8 kg C/year according to the Hestia results, 69 times the value reported by ODIAC (4.87×10^6 kg C/year).

There are also occurrences in which a grid cell with a large GRD value contained large emissions for only one of the two approaches, resulting in order-of-magnitude differences. Examples associated with this type of difference include the Citizens Thermal facility (Indianapolis −86.16, 39.76), in which Hestia reports a grid cell value (2.14×10^8 kg C/year) 56 times the magnitude reported by ODIAC (3.81×10^6 kg C/year). Given that no large emitting grid cells were identified in the vicinity of the paired ODIAC grid cell, this suggests that the Citizens Thermal facility was missing in the ODIAC FFCO$_2$ emission results.
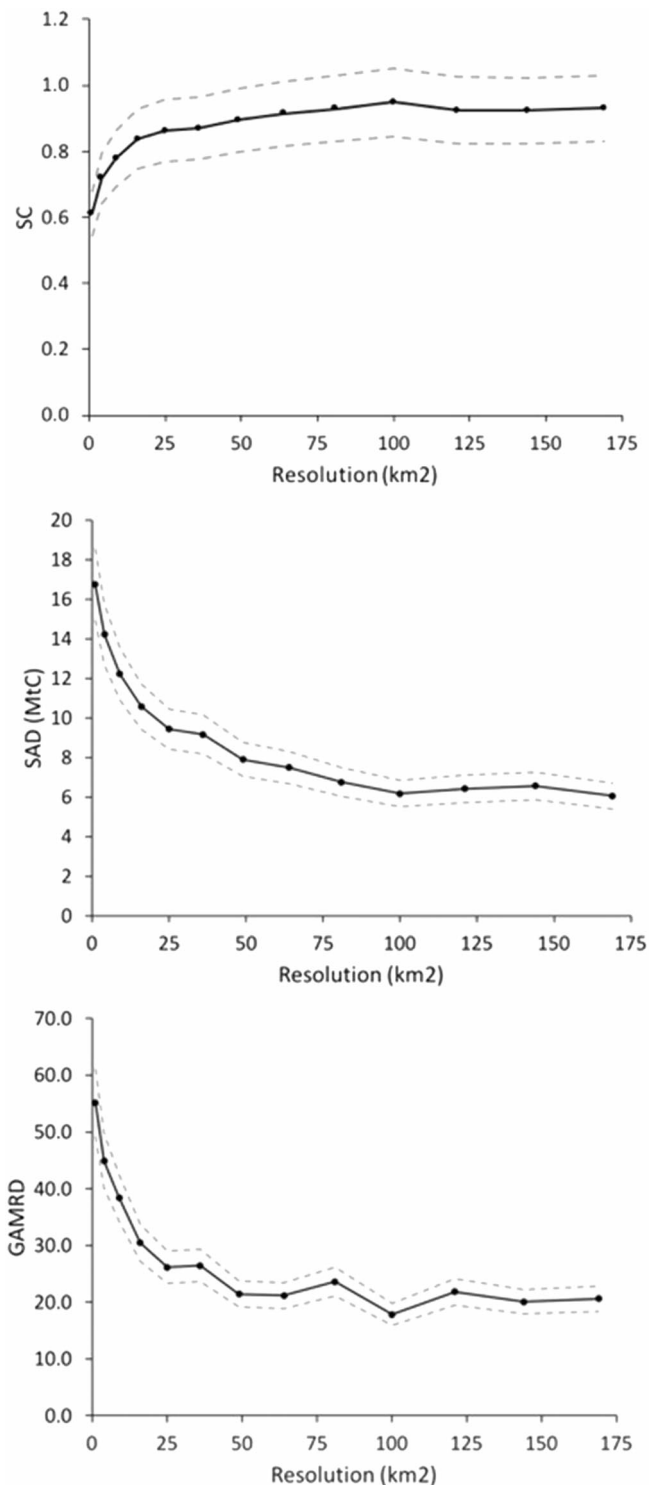
Figure 6. Three spatial difference metrics between ODIAC and Hestia annual $FFCO_2$ emissions versus spatial resolution in the Los Angeles Basin urban area. (a) Spatial correlation (SC), (b) summed absolute difference (SAD), and (c) grid cell median absolute percentage difference (GAMRD). All are calculated for emission accumulations less than 90% of city total (see Figure 5).

4. Discussion

The whole-city differences between the global gridded downscaled and bottom-up $FFCO_2$ emission data products compared here range from less than 2% in the Los Angeles Basin to over 20% in Salt Lake City. Given the areal extent of the Los Angeles Basin (17,795 km^2) relative to the other three cities (405 to 3,190 km^2), this may be consistent with the increased agreement as resolution is coarsened and countervailing differences averaged. As U.S. cities are concerned, however, Los Angeles is an outlier in terms of size, ranking as the seventh largest metropolitan area by areal extent and second by population (https://en.wikipedia.org/wiki/List_of_ United_States_urban_areas). Hence, cities of smaller areal extent, not unlike Baltimore, Salt Lake City, and Indianapolis, are the norm rather than the exception in the United States. The whole-city differences in these more common city sizes, ranging from the 10 to 20%, found here imply that, while midcentury CO_2 reduction goals pledged by many U.S. cities may be amenable to scientific assessment, near-term "course-correction" or individual policy assessment, will be challenging. The utility of the two approaches in policy application will rest on the balance between the cost of development and the benefits of accuracy. It is worth noting that the cost- and labor-intensiveness of the bottom-up approaches will continue to be reduced as more learning and automation are achieved or more scientifically driven methodologies are adopted by cities in place of self-reported efforts. Similarly, with more comparison studies and incorporation of a more diverse set of downscaling proxies or hybrid methods, global data products may see improvements in accuracy. Nevertheless, the differences found in this study at the whole-city scale leaves one optimistic as they are far less than the differences identified at smaller spatial scales.

The differences in spatial distribution at the subcity scales are much larger and raise greater concern given the importance of high-resolution spatially explicit estimates of urban $FFCO_2$ emissions to both science and policy. The most pronounced sector-specific spatial difference found in this study, aside from individual point source discrepancies, is that associated with on-road $FFCO_2$ emissions (Figure 3). This is best exemplified by the emission differences in Indianapolis, particularly associated with the interstate circling the city of Indianapolis (I-465). Grid cells in which on-road emissions account for more than 90% of the grid cell total were identified and the percent relative difference of these accumulated emissions calculated (table in the supporting information). The Hestia on-road $FFCO_2$ emissions in these instances were larger than ODIAC in three out of four cities. For example, in the Los Angeles Basin, Indianapolis, and Salt Lake City, the Hestia emissions are 51.6, 57.3, and 8.1% larger than ODIAC, respectively. In Baltimore, by contrast, Hestia emissions are 166.8% smaller than ODIAC, although only 24 on-road-dominated grid cells were identified in this city.

The Hestia $FFCO_2$ emission estimation approach explicitly quantifies the spatial distribution of on-road $FFCO_2$ emissions using roadway basemap information and traffic monitoring. The ODIAC distribution of $FFCO_2$ emissions by nighttime lights does not specifically allocate emissions to roads unless they have significant proximal lighting such as associated with dense building clusters (e.g., commercial hubs). Therefore, it is not surprising that grid cells containing significant on-road emissions have

larger values than the counterpart ODIAC grid cells for which lighting is a suboptimal roadway spatial proxy. The exception in Baltimore is likely due to urban boundary encompassing only the most populated and commercially dense portions of the larger urban area, and hence, the roads are proximal to greater levels of lighting.

Similarly, the narrower range of FFCO$_2$ emission values across the entirety of the urban areas (Figures 2 and 4) in the ODIAC versus Hestia results reflects a limitation of both the low-end sensitivity and saturation of nighttime lights restricting the lower and upper extent of radiance values. Hence, downscaling national/regional total emissions in proportion to nightlight radiance values will be restricted by nightlight saturation effects (Levin & Duke, 2012), and this will be imputed to the FFCO$_2$ emission estimation.

As point sources constitute a large proportion of the global FFCO$_2$ emission budget, they are critical to mitigation policymaking. In the United States, for example, power plant emissions, alone, represent roughly 40% of the national FFCO$_2$ emission budget (Pétron et al., 2008) and have been the target of national policy (Federal Register, 2015). Point sources such as industrial facilities and airports can also be major contributors to FFCO$_2$ emissions. For example, industrial facilities and airports, respectively, contributed 3.1 and 4.8% of the total FFCO$_2$ emissions in Indianapolis (Gurney et al., 2012). Large point source emitters, other than those supplied with bottom-up databases (i.e., the CARMA database used by ODIAC), are currently difficult to characterize comprehensively using downscaling techniques because of their small areal footprint. Furthermore, many point sources do not have lighting intensity commensurate with their FFCO$_2$ emission magnitude. The comparison of large emissions with large GRD values supports this argument.

The large GRD values that occur in Baltimore's Inner Harbor area (occupying about 10% of the total Baltimore city area) are associated with commercial marine vessel FFCO$_2$ emissions and account for 8.4% of the Baltimore FFCO$_2$ emission total. The Hestia emissions explicitly place commercial marine vessel FFCO$_2$ emissions into a combination of a port polygon and polyline shipping lane spatial entities. Nighttime lights will not capture the magnitude or spatial distribution of these commercial marine vessel emissions associated with the port activity, particularly the shipping lane delineation, to the extent that they are not accompanied by lighting intensity commensurate with their FFCO$_2$ emissions.

Although differences are readily evident at the finest spatial resolution available in the two approaches (1 km^2), agreement steadily improves as the resolution is coarsened. Furthermore, although there is no single threshold beyond which agreement can be stated unequivocally, the improvement in agreement slows beyond roughly 25 km^2 (5 km × 5 km) to 100 km^2 (10 km × 10 km), depending upon the metric of agreement used. This suggests the spatial scale at which the distribution error, incurred with downscaling approaches is minimized. However, additional work is needed to examine this relationship beyond the four U.S. cities included in this study.

The application of FFCO$_2$ emission data products in science and policy place a burden on generating the most accurate space/time-resolved FFCO$_2$ emissions with an objectively informed uncertainty. Both of these goals remain challenging. Although accuracy can be assessed through comparison to independent methods, notably atmospheric CO$_2$ inversions, quantification of uncertainty remains difficult owing to the nature of the data sources typically relied upon in constructing space/time-resolved FFCO$_2$ emission data products. Comparisons, such as carried out here, offer a form of uncertainty assessment.

The demand for accuracy and uncertainty quantification in FFCO$_2$ emission data products will only increase as subnational governments increase their involvement in climate change greenhouse gas emission mitigation. For example, 9,120 cities representing over 770 million people (10.5% of global population) have committed to the Global Covenant of Mayors to promote and support action to combat climate change (Global Covenant of Mayors (GCoM), 2018). Over 90 megacities, as part of the C40 network, have similarly committed to mitigation actions with demonstrable progress. In the United States, over 400 cities have pledged to meet or exceed the U.S. target under the Paris Accords of the United Nations Climate Change Negotiation (Watts, 2017; Madhani, 2017; climatemayors.org/). Cities have set specific emission reduction targets including specific timelines and sector-specific regulatory policies (Trencher et al., 2016; Ürge-Vorsatz et al., 2018). For example, the City of New York has committed under the Greener, Greater Buildings Plan to reduce emissions to 80% below 2005 levels by 2050. The City of San Francisco has committed to the same reduction target under the Existing Commercial Buildings Energy Performance Ordinance.

These reduction targets will have to be operationalized through specific policies that direct resources to specific instruments such as retrofitting building envelopes, adding high-occupancy vehicle lanes, or adding/improving mass transit infrastructure. In nearly all of these instances, there is a need for spatially and temporally resolved information to most efficiently target those elements within the emitting landscape that account for the largest share of emissions. In the typically logarithmically distributed $FFCO_2$ emissions in a city (few emitters account for a large share of emissions), identifying these emitters and understanding their spatial and temporal relationship to each other and other important attributes such as income or traffic congestion is critical to policy efficiency. The space and time scales relevant are down to the individual building and road segment for every hour (to resolve, for example, rush hours). Policy efficiency will soon emerge as a critical need as cities approach their reduction target time horizons and resources are allocated to mitigate emissions, such as is now occurring in the state of California (New York Times, 2017).

Both the downscaling and bottom-up urban $FFCO_2$ estimation approaches face challenges in quantifying their respective emission uncertainty and one must exercise caution in interpreting the differences between the two approaches compared here as a definitive form of uncertainty. It offers a rough guide and rests, to a certain extent, on the veracity of the bottom-up Hestia $FFCO_2$ emission data product. It appears reasonable to assume that the Hestia $FFCO_2$ emission approach represents urban-scale emission spatial distribution more accurately due to the more accurate spatio-physical representation of emitting elements (e.g., roads, industrial facilities, buildings). The Hestia $FFCO_2$ emission magnitude may also represent a more accurate estimate based on close agreement between the Hestia emissions in Indianapolis and an urban-scale atmosphere CO_2 inversion estimate (Gurney et al., 2017). However, acknowledging the internal uncertainty and the fact that there has been limited comparison to independent methods suggests that an assumption that Hestia provides an unbiased quantification of $FFCO_2$ emissions be adopted with caution.

Both approaches will continue to be valuable to the increasing scientific and policy needs associated with quantification of urban $FFCO_2$ fluxes. Both approaches have strengths and weaknesses which make them alternatively useful in differing contexts. While the bottom-up approach may offer a great amount of information with more location accuracy, it comes at a cost in terms of data gathering, data analysis, and idiosyncratic conditions in individual cities. Downscaling efforts, by contrast, can generate resolved $FFCO_2$ estimates across the planet in a single effort but must use spatial proxies which can fail, to varying degrees, to match the emitting processes estimated. The trade-off is the cost versus emission estimation accuracy at scales considered effective for the increasingly important question of policy efficiency.

With these caveats in mind, we can return to the questions posed at the outset of this study. Given the differences found here, a "proxy" uncertainty of the downscaled approach, using the ODIAC data product as the example effort, ranges from 47 to 84%, depending upon city, at the 1-km^2 spatial resolution. At the whole-city scale, agreement is much improved, particularly for the Los Angeles Basin (−1.52%). For the three remaining cities, we find differences of 10.7% (Baltimore), 12.5% (Indianapolis), and 20.8% (Salt Lake City). Agreement between the two approaches compared here improves when the resolution is lessened via aggregation and there appears to be a diminishing return to resolution coarsening in the 25- to 100-km^2 range. Opportunities for improving agreement between the downscaling and bottom-up approaches are most significant in better representing the spatial and magnitude characteristics of on-road $FFCO_2$ emissions in the downscaled approaches for which roads remain poorly represented spatially by coarse proxies. Furthermore, improvement in the representation of point sources, whose emissions do not scale linearly with proxies such as lighting or population, offer similar opportunities for improvement and may be available for large portions of the world via national databases on local air pollution or even the use of high-resolution visible/thermal imagery.

5. Conclusions

This comparison of a simple downscaled (ODIAC) fossil fuel CO_2 ($FFCO_2$) emission data product to a bottom-up (Hestia) $FFCO_2$ emission data product in four U.S. cities shows differences in terms of whole-city emission magnitude, grid cell-scale estimates, and spatial distribution. Whole-city differences range from a minimum of −1.5% in the Los Angeles Basin to a maximum of 20.8% in Salt Lake City. Given the range of city size and characteristics, this constitutes good agreement at these scales. At the scale of individual 1-km^2 grid cells, the relative differences were larger, ranging from 47 to 84% for the four cities and spatial

correlations ranging from 0.34 to 0.68. Among the reasons for the grid cell differences, the nightlight low-end sensitivity and saturation effects are likely large contributors. Limited sectoral separation in applying spatial proxies in the downscaling approach leads to inaccurate spatial distribution in emissions, particularly in the case of on-road $FFCO_2$ emissions, often a dominant portion of urban $FFCO_2$. Finally, uncertainty in the geo-location of large point sources can lead to large biases in the grid cell-scale $FFCO_2$ estimation and account for a significant proportion of the spatial differences. The two approaches to estimating urban $FFCO_2$ have unique strengths and weaknesses. Downscaling approaches typically estimate emissions for regional to global scales efficiently, offering quantification for many cities. Bottom-up approaches, by contrast, are more labor intensive and are incrementally produced, city-by-city. By aggregating the resolution of the downscaling emission data product used in this study, reasonable agreement was achieved between the two approaches at a spatial resolution beyond 25 km^2. This may offer guidance to practical use of downscaling approaches when applied to urban $FFCO_2$ scientific or policy problems.

References

Andres, R. J., Boden, T. A., Bréon, F., Ciais, P., Davis, S., Erickson, D., et al. (2012). A synthesis of carbon dioxide emissions from fossil-fuel combustion. *Biogeosciences Discussions*, 9(1), 1299–1376. https://doi.org/10.5194/bgd-9-1299-2012

Andres, R. J., Boden, T. A., & Higdon, D. M. (2016). Gridded uncertainty in fossil fuel carbon dioxide emission maps, a CDIAC example. *Atmospheric Chemistry and Physics*, 16(23), 14,979–14,995. https://doi.org/10.5194/acp-16-14979-2016, https://doi.org/10.5194/acp-16-14979-2016

Andres, R. J., Fielding, D. J., Marland, G., Boden, T. A., Kumar, N., & Kearney, A. T. (1999). Carbon dioxide emissions from fossil fuel use, 1751–1950. *Tellus Series B: Chemical and Physical Meteorology*, 51(4), 759–765. https://doi.org/10.1034/j.1600-0889.1999.t01-3-00002.x

Andres, R. J., Marland, G., Fung, I., & Matthews, E. (1996). A 1° × 1° distribution of carbon dioxide emissions from fossil fuel consumption and cement manufacture, 1950–1990. *Global Biogeochemical Cycles*, 10(3), 419–429. https://doi.org/10.1029/96GB01523

Asefi-Najafabady, S., Rayner, P. J., Gurney, K. R., McRobert, A., Song, Y., Coltin, K., & Baugh, K. (2014). A multiyear, global gridded fossil fuel CO_2 emission data product: Evaluation and analysis of results. *Journal of Geophysical Research: Atmospheres*, 119, 10,213–10,231. https://doi.org/10.1002/2013JD021296

Boden, T. A., Marland, G., & Andres, R. J. (1995). Estimates of global, regional, and national annual CO_2 emissions from fossil-fuel burning, hydraulic cement production, and gas flaring: 1950–1992. ORNL/CDIAC-90, NDP-30/R6. Oak Ridge, TN: Oak Ridge National Laboratory, U.S. Department of Energy.

Boden, T. A., Marland, G., & Andres, R. J. (2013). *Global, Regional, and National Fossil-Fuel CO_2 Emissions* (Vol. 53, pp. 1689–1699). Oak Ridge, TN: Carbon Dioxide Information Analysis Center, Oak Ridge National Laboratory, U.S. Department of Energy. https://doi.org/10.3334/CDIAC/00001_V2013

Boden, T. A., Marland, G., & Andres, R. J. (2017). *Global, Regional, and National Fossil-Fuel CO_2 Emissions* (Vol. 53, pp. 1689–1699). Oak Ridge, TN: Carbon Dioxide Information Analysis Center, Oak Ridge National Laboratory, U.S. Department of Energy. https://doi.org/10.3334/CDIAC/00001_V2017

Brioude, J., Angevine, W. M., Ahmadov, R., Kim, S. W., Evan, S., McKeen, S. A., et al. (2013). Top-down estimate of surface flux in the Los Angeles Basin using a mesoscale inverse modeling technique: Assessing anthropogenic emissions of CO, NO_x and CO_2 and their impacts. *Atmospheric Chemistry and Physics*, 13(7), 3661–3677. https://doi.org/10.5194/acp-13-3661-2013

Brondfield, M. N., Hutyra, L. R., Gately, C. K., Raciti, S. M., & Peterson, S. a. (2012). Modeling and validation of on-road CO_2 emissions inventories at the urban regional scale. *Environmental Pollution*, 170, 113–123. https://doi.org/10.1016/j.envpol.2012.06.003

Bulkeley, H. (2010). Cities and the governing of climate change. *Annual Review of Environment and Resources*, 35(1), 229–253. https://doi.org/10.1146/annurev-environ-072809-101747

Doll, C. H., Muller, J.-P., & Elvidge, C. D. (2000). Night-time imagery as a tool for global mapping of socioeconomic parameters and greenhouse gas emissions. *Ambio: A Journal of the Human Environment*, 29(3), 157–162. https://doi.org/10.1579/0044-7447-29.3.157

Duren, R. M., & Miller, C. E. (2012). Measuring the carbon emissions of megacities. *Nature Climate Change*, 2(8), 560–562. https://doi.org/10.1038/nclimate1629

Engelen, R. J., Denning, A. S., & Gurney, K. R. (2002). On error estimation in atmospheric CO_2 inversions. *Journal of Geophysical Research*, 107(D22), 4635. https://doi.org/10.1029/2002JD002195

Enting, I. (2002). *Inverse Problems in Atmospheric Constituent Transport*. New York: Cambridge University Press. https://doi.org/10.1017/CBO9780511535741

Erickson, D. J., Mills, R. T., Gregg, J., Blasing, T. J., Hoffman, F. M., Andres, R. J., et al. (2008). An estimate of monthly global emissions of anthropogenics CO_2: Impact on the seasonal cycle of atmospheric CO_2. *Journal of Geophysical Research*, 113, G01023. https://doi.org/10.1029/2007JG000435

Federal Register (2015). 40 CFR Part 60, Carbon Pollution Emission Guidelines for Existing Stationary Sources: Electric Utility Generating Units; Final Rule Environmental Protection Agency.

Feng, S., Lauvaux, T., Newman, S., Rao, P., Ahmadov, R., Deng, A., et al. (2016). Los Angeles megacity: A high-resolution land-atmosphere modelling system for urban CO_2 emissions. *Atmospheric Chemistry and Physics*, 16(14), 9019–9045. https://doi.org/10.5194/acp-16-9019-2016

Gately, C. K., & Hutyra, L. R. (2017). Large uncertainties in urban-scale carbon emissions. *Journal of Geophysical Research: Atmospheres*, 122, 11,242–11,260. https://doi.org/10.1002/2017JD027359

Gately, C. K., Hutyra, L. R., Wing, I. S., & Brondfield, M. N. (2013). A bottom up approach to on-road CO_2 emissions estimates: Improved spatial accuracy and applications for regional planning. *Environmental Science and Technology*, 47(5), 2423–2430. https://doi.org/10.1021/es304238v

Ghosh, T., Elvidge, C. D., Sutton, P. C., Baugh, K. E., Ziskin, D., & Tuttle, B. T. (2010). Creating a global grid of distributed fossil fuel CO_2 emissions from nighttime satellite imagery. *Energies*, 3(12), 1895–1913. https://doi.org/10.3390/en3121895

Global Covenant of Mayors (GCoM) (2018). https://www.globalcovenantofmayors.org/

Goodfriend, W., Reyes, B., & Pac, S. (2017). 2015 San Francisco Geographic Greenhouse Gas Emissions Inventory at a Glance, San Francisco Department of Environment, Climate Program. Retrieved from https://sfenvironment.org/sites/default/files/fliers/files/sfe_cc_2015_community_inventory_report.pdf (accessed August 31, 2018).

Gregg, J. S., & Andres, R. J. (2008). A method for estimating the temporal and spatial patterns of carbon dioxide emissions from national fossil-fuel consumption. *Tellus Series B: Chemical and Physical Meteorology*, *60*(B1), 1–10. https://doi.org/10.1111/j.1600-0889.2007.00319.x

Gregg, J. S., Losey, L. M., Andres, R. J., Blasing, T. J., & Marland, G. (2009). The temporal and spatial distribution of carbon dioxide emissions from fossil-fuel use in North America. *Journal of Applied Meteorology and Climatology*, *48*(12), 2528–2542. https://doi.org/10.1175/2009JAMC2115.1

Gurney, K. R. (2014). The urban landscape: Recent research quantifying carbon emissions down to the street level. *Carbon Management*, *5*(3), 309–320. https://doi.org/10.1080/17583004.2014.986849

Gurney, K. R., Chen, Y. H., Maki, T., Kawa, S. R., Andrews, A., & Zhu, Z. (2005). Sensitivity of atmospheric CO_2 inversions to seasonal and interannual variations in fossil fuel emissions. *Journal of Geophysical Research*, *110*, D10308. https://doi.org/10.1029/2004JD005373

Gurney, K. R., Huang, J., & Coltin, K. (2016). Bias present in US federal agency power plant CO_2 emissions data and implications for the US clean power plan. *Environmental Research Letters*, *11*(6). https://doi.org/10.1088/1748-9326/11/6/064005

Gurney, K. R., Law, R. M., Denning, A. S., Rayner, P. J., Baker, D., Bousquet, P., et al. (2002). Towards robust regional estimates of CO_2 sources and sinks using atmospheric transport models. *Nature*, *415*(6872), 626–630. https://doi.org/10.1038/415626a

Gurney, K. R., Liang, J., Patarasuk, R., O'Keeffe, D., Huang, J., Hutchins, M., et al. (2017). Reconciling the differences between a bottom-up and inverse-estimated FFCO$_2$ emissions estimate in a large US urban area. *Elementa: Science of the Anthropocene*, *5*(0), 44. https://doi.org/10.1525/elementa.137

Gurney, K. R., Mendoza, D. L., Zhou, Y., Fischer, M. L., Miller, C. C., Geethakumar, S., & de la Rue du Can, S. (2009). High resolution fossil fuel combustion CO_2 emission fluxes for the United States. *Environmental Science & Technology*, *43*(14), 5535–5541. https://doi.org/10.1021/es900806c

Gurney, K. R., Razlivanov, I., Song, Y., Zhou, Y., Benes, B., & Abdul-Massih, M. (2012). Quantification of fossil fuel CO_2 emissions on the building/street scale for a large U.S. City. *Environmental Science and Technology*, *46*(21), 12,194–12,202. https://doi.org/10.1021/es3011282

Gurney, K. R., Romero-Lankao, P., Seto, K. C., Hutyra, L. R., Duren, R., Kennedy, C., et al. (2015). Climate change: Track urban emissions on a human scale. *Nature*, *525*(7568), 179–181. https://doi.org/10.1038/525179a

Hartmann, D. (1998). Global warming: The complete briefing. *Eos, Transactions of the American Geophysical Union*, *79*(33), 396. https://doi.org/10.1029/98EO00304

Hogue, S., Marland, E., Andres, R. J., Marland, G., & Woodard, D. (2016). Uncertainty in gridded CO_2 emissions estimates. *Earth's Future*, *4*, 225–239. https://doi.org/10.1002/2015EF000343

Hsu, A., Moffat, A. S., Weinfurter, A. J., & Schwartz, J. D. (2015). Towards a new climate diplomacy. *Nature Climate Change*, *5*(6), 501–503. https://doi.org/10.1038/nclimate2594

Hsu, A., Weinfurter, A. J., & Xu, K. (2017). Aligning subnational climate actions for the new post-Paris climate regime. *Climatic Change*, *142*(3–4), 419–432. https://doi.org/10.1007/s10584-017-1957-5

Hutchins, M. G., Colby, J. D., Marland, G., & Marland, E. (2016). A comparison of five high-resolution spatially-explicit, fossil-fuel, carbon dioxide emission inventories for the United States. *Mitigation and Adaptation Strategies for Global Change*, *22*(6), 947–972. https://doi.org/10.1007/s11027-016-9709-9

Hutyra, L. R., Duren, R., Gurney, K. R., Grimm, N., Kort, E. A., Larson, E., & Shrestha, G. (2014). Urbanization and the carbon cycle: Current capabilities and research outlook from the natural sciences perspective. *Earth's Future*, *2*, 473–495. https://doi.org/10.1002/2014EF000255

Janssens-Maenhout, G., Dentener, F., van Aardenne, J., Monni, S., Pagliari, V., Orlandini, L., et al. (2012). EDGAR-HTAP: A harmonized gridded air pollution emission dataset based on national inventories, JRC scientific and technical reports, EUA 25229 EN-2012.

Jones, C., & Kammen, D. M. (2014). Spatial distribution of U.S. household carbon footprints reveals suburbanization undermines greenhouse gas benefits of urban population density. *Environmental Science and Technology*, *48*(2), 895–902. https://doi.org/10.1021/es4034364

Kennedy, C., Steinberger, J., Gasson, B., Hansen, Y., Hillman, T., Havranek, M., et al. (2009). Greenhouse gas emissions from global cities. *Environmental Science & Technology*, *43*(19), 7297–7302. Retrieved from http://www.ncbi.nlm.nih.gov/pubmed/19848137, https://doi.org/10.1021/es900213p

Lauvaux, T., Miles, N. L., Deng, A., Richardson, S. J., Cambaliza, M. O., Davis, K. J., et al. (2016). High-resolution atmospheric inversion of urban CO_2 emissions during the dormant season of the Indianapolis flux experiment (INFLUX). *Journal of Geophysical Research: Atmospheres*, *121*, 5213–5236. https://doi.org/10.1002/2015JD024473

Le Quéré, C., Andres, R. J., Boden, T., Conway, T., Houghton, R. A., House, J. I., et al. (2013). The global carbon budget 1959–2011. *Earth System Science Data*, *5*(1), 165–185. https://doi.org/10.5194/essd-5-165-2013

Levin, N., & Duke, Y. (2012). High spatial resolution night-time light images for demographic and socio-economic studies. *Remote Sensing of Environment*, *119*, 1–10. https://doi.org/10.1016/j.rse.2011.12.005

Liang, J., Gurney, K. R., O'Keeffe, D., Hutchins, M., Patarasuk, R., Huang, J., et al. (2017). Optimizing the spatial resolution for urban CO_2 flux studies using the Shannon entropy. *Atmosphere*, *8*(12). https://doi.org/10.3390/atmos8050090

Liu, J., Bowman, K., Schimel, D., Parazoo, N., Jiang, Z., Lee, M., et al. (2017). Contrasting carbon cycle responses of the tropical continents to the 2015–2016 El Niño. *Science*, *358*(6360), eaam5690. https://doi.org/10.1126/science.aam5690

Macknick, J. (2011). Energy and CO_2 emission data uncertainties. *Carbon Management*, *2*(2), 189–205. https://doi.org/10.4155/cmt.11.10

Madhani, A. (2017). Forget Paris: U.S. mayors sign their own pact after Trump ditches climate accord. *USA Today*.

Marland, G., Rotty, R. M., & Treat, N. L. (1985). CO_2 from fossil fuel burning: Global distribution of emissions. *Tellus B*, *37B*(4–5), 243–258. https://doi.org/10.1111/j.1600-0889.1985.tb00073.x

McKain, K., Wofsy, S. C., Nehrkorn, T., Eluszkiewicz, J., Ehleringer, J. R., & Stephens, B. B. (2012). Assessment of ground-based atmospheric observations for verification of greenhouse gas emissions from an urban region. *Proceedings of the National Academy of Sciences*, *109*(22), 8423–8428. https://doi.org/10.1073/pnas.1116645109

Mitchell, L. E., Lin, J. C., Bowling, D. R., Pataki, D. E., Strong, C., Schauer, A. J., et al. (2018). Long-term urban carbon dioxide observations reveal spatial and temporal dynamics related to urban characteristics and growth. *Proceedings of the National Academy of Sciences of the United States of America*, *115*(12), 2912–2917. https://doi.org/10.1073/pnas.1702393115

Nassar, R., Napier-Linton, L., Gurney, K. R., Andres, R. J., Oda, T., Vogel, F. R., & Deng, F. (2013). Improving the temporal and spatial distribution of CO_2 emissions from global fossil fuel emission data sets. *Journal of Geophysical Research: Atmospheres*, *118*, 917–933. https://doi.org/10.1029/2012JD018196

New York Times (2017). U.S. Climate Change Policy: Made in California, The New York Times, September 27, 2017. Retrieved from https://www.nytimes.com/2017/09/27/climate/california-climate-change.html

Newman, S., Xu, X., Gurney, K. R., Hsu, Y. K., Li, K. F., Jiang, X., et al. (2016). Toward consistency between trends in bottom-up CO_2 emissions and top-down atmospheric measurements in the Los Angeles megacity. *Atmospheric Chemistry and Physics*, *16*(6), 3843–3863. https://doi.org/10.5194/acp-16-3843-2016

Oda, T., Lauvaux, T., Lu, D., Rao, P., Miles, N. L., Richardson, S. J., & Gurney, K. R. (2017). On the impact of granularity of space-based urban CO_2 emissions in urban atmospheric inversions: A case study for Indianapolis, IN. *Elementa*, *5*(28). http://doi.org/10.1525/elementa.146

Oda, T., & Maksyutov, S. (2011). A very high-resolution (1 km × 1 km) global fossil fuel CO_2 emission inventory derived using a point source database and satellite observations of nighttime lights. *Atmospheric Chemistry and Physics*, *11*(2), 543–556. https://doi.org/10.5194/acp-11-543-2011

Oda, T., Maksyutov, S., & Andres, R. J. (2018). The Open-source Data Inventory for Anthropogenic CO_2, version 2016 (ODIAC2016): A global monthly fossil fuel CO_2 gridded emissions data product for tracer transport simulations and surface flux inversions. *Earth System Science Data*, *10*(1), 87–107. https://doi.org/10.5194/essd-10-87-2018

Olivier, J. G. J., Bloos, J. P. J., Berdowski, J. J. M., Visschedijk, A. J. H., & Bouwman, A. F. (1999). A 1990 global emission inventory of anthropogenic sources of carbon monoxide on 1° × 1° developed in the framework of EDGAR/GEIA. *Chemosphere - Global Change Science*, *1*(1–3), 1–17. https://doi.org/10.1016/S1465-9972(99)00019-7

Ou, J., Liu, X., Li, X., Li, M., & Li, W. (2015). Evaluation of NPP-VIIRS nighttime light data for mapping global fossil fuel combustion CO_2 emissions: A comparison with DMSP-OLS nighttime light data. *PLoS One*, *10*(9), e0138310. https://doi.org/10.1371/journal.pone.0138310

Parshall, L., Gurney, K., Hammer, S. A., Mendoza, D., Zhou, Y., & Geethakumar, S. (2010). Modeling energy consumption and CO_2 emissions at the urban scale: Methodological challenges and insights from the United States. *Energy Policy*, *38*(9), 4765–4782. https://doi.org/10.1016/j.enpol.2009.07.006

Patarasuk, R., Gurney, K. R., O'Keeffe, D., Song, Y., Huang, J., Rao, P., et al. (2016). Urban high-resolution fossil fuel CO_2 emissions quantification and exploration of emission drivers for potential policy applications. *Urban Ecosystems*, *19*(3), 1013–1039. https://doi.org/10.1007/s11252-016-0553-1

Pétron, G., Tans, P., Frost, G., Chao, D., & Trainer, M. (2008). High-resolution emissions of CO_2 from power generation in the USA. *Journal of Geophysical Research*, *113*, G04008. https://doi.org/10.1029/2007JG000602

Pincetl, S., Chester, M., Circella, G., Fraser, A., Mini, C., Murphy, S., et al. (2014). Enabling future sustainability transitions: An urban metabolism approach to Los Angeles Pincetl et al. Enabling Future Sustainability Transitions. *Journal of Industrial Ecology*, *18*(6), 871–882. https://doi.org/10.1111/jiec.12144

Porse, E., Derenski, J., Gustafson, H., Elizabeth, Z., & Pincetl, S. (2016). Structural, geographic, and social factors in urban building energy use: Analysis of aggregated account-level consumption data in a megacity. *Energy Policy*, *96*, 179–192. https://doi.org/10.1016/j.enpol.2016.06.002

Ramaswami, A., Hillman, T., Janson, B., Reiner, M., & Thomas, G. (2008). A demand-centered, hybrid life-cycle methodology for city-scale greenhouse gas inventories. *Environmental Science and Technology*, *42*(17), 6455–6461. https://doi.org/10.1021/es702992q

Rayner, P. J., Raupach, M. R., Paget, M., Peylin, P., & Koffi, E. (2010). A new global gridded data set of CO_2 emissions from fossil fuel combustion: Methodology and evaluation. *Journal of Geophysical Research*, *115*, D19306. https://doi.org/10.1029/2009JD013439

Rosenzweig, C., Solecki, W., Hammer, S. A., & Mehrotra, S. (2010). Cities lead the way in climate-change action. *Nature*, *467*(7318), 909–911. https://doi.org/10.1038/467909a

Schuh, A. E., Denning, A. S., Corbin, K. D., Baker, I. T., Uliasz, M., Parazoo, N., et al. (2010). A regional high-resolution carbon flux inversion of North American for 2004. *Biogeosciences*, *7*(5), 1625–1644. https://doi.org/10.5194/bg-7-1625-2010

Seto, K., Bigio, A., Blanco, H., Delgado, G. C., Dewar, D., Huang, L., et al. (2015). Mitigation of climate change. In C. B. Field et al. (Eds.), *Climate Change 2014: Impacts, Adaptation, and Vulnerability. Part A: Global and Sectoral Aspects. Contribution of Working Group II to the Fifth Assessment Report of the Intergovernmental Panel on Climate Change* (pp. 361–409). United Kingdom and New York, NY: Cambridge University Press.

Shiga, Y. P., Michalak, A. M., Gourdji, S. M., Mueller, K. L., & Yadav, V. (2014). Detecting fossil fuel emissions patterns from subcontinental regions using North American in situ CO_2 measurements. *Geophysical Research Letters*, *41*, 4381–4388. https://doi.org/10.1002/2014GL059684

Shu, Y., & Lam, N. S. N. (2011). Spatial disaggregation of carbon dioxide emissions from road traffic based on multiple linear regression model. *Atmospheric Environment*, *45*(3), 634–640. https://doi.org/10.1016/J.ATMOSENV.2010.10.037

Trencher, G., Castán Broto, V., Takagi, T., Sprigings, Z., Nishida, Y., & Yarime, M. (2016). Innovative policy practices to advance building energy efficiency and retrofitting: Approaches, impacts and challenges in ten C40 cities. *Environmental Science and Policy*, *66*, 353–365. https://doi.org/10.1016/j.envsci.2016.06.021

Turnbull, J. C., Sweeney, C., Karion, A., Newberger, T., Lehman, S. J., Tans, P. P., et al. (2015). Toward quantification and source sector identification of fossil fuel CO_2 emissions from an urban area: Results from the INFLUX experiment. *Journal of Geophysical Research: Atmospheres*, *120*, 292–312. https://doi.org/10.1002/2014JD022555

Ummel, K. (2012). Carma revisited: An updated database of carbon dioxide emissions from power plants worldwide (August 23, 2012), Center for Global Development Working Paper No. 304. Available at SSRN: https://ssrn.com/abstract=2226505 or https://doi.org/10.2139/ssrn.2226505

United States Environmental Protection Agency (2017). Inventory of U.S. greenhouse gas emissions and sinks 1990–2015, EPA 430-P-17-001.

Ürge-Vorsatz, D., Rosenzweig, C., Dawson, R. J., Rodriguez, R. S., Bai, X., Barau, A. S., et al. (2018). Locking in positive climate responses in cities. *Nature Climate Change*, *8*(3), 174–177, https://doi.org/10.1038/s41558-018-0100-6

Vandeweghe, J. R., & Kennedy, C. (2007). A spatial analysis of residential greenhouse gas emissions in the Toronto census metropolitan area. *Journal of Industrial Technology*, *11*(2).

Wang, R., Tao, S., Ciais, P., Shen, H. Z., Huang, Y., Chen, H., et al. (2013). High-resolution mapping of combustion processes and implications for CO_2 emissions, *Atmos. Chem. Phys.*, 13, 5189-5203Watts, M. (2017) cities spearhead climate action. *Nature Climate Change*, 7, 537–538.

Watts, M. (2017). Cities spearhead climate action. *Nature Climate Change*, 7, 937–938.

Wu, L., Broquet, G., Ciais, P., Bellassen, V., Vogel, F., Chevallier, F., et al. (2016). What would dense atmospheric observation networks bring to the quantification of city CO_2 emissions? *Atmospheric Chemistry and Physics*, *16*(12), 7743–7771. https://doi.org/10.5194/acp-16-7743-2016

Zhang, X., Gurney, K. R., Rayner, P., Baker, D., & Liu, Y.-P. (2015). Sensitivity of simulated CO_2 concentration to sub-annual variations in fossil fuel CO_2 emissions. *Atmospheric Chemistry and Physics Discussions*, *15*(14), 20,679–20,708. https://doi.org/10.5194/acpd-15-20679-2015

Zhao, T., Horner, M. W., & Sulik, J. (2011). A geographic approach to sectoral carbon inventory: Examining the balance between consumption-based emissions and land-use carbon sequestration in Florida. *Annals of the Association of American Geographers*, *101*(4), 752–763. https://doi.org/10.1080/00045608.2011.567936

Zhou, Y., & Gurney, K. (2010). A new methodology for quantifying on-site residential and commercial fossil fuel CO_2 emissions at the building spatial scale and hourly time scale. *Carbon Management*, *1*(1), 45–56. https://doi.org/10.4155/cmt.10.7